DE-FG22-94PC94224--14

High Temperature Alkali Corrosion of Sense SN_4 Coated with CMZP and Mg-Doped A_21TiO_5 In Coal Gas

Topical Report
November 1, 1997 - March 1, 1998

By
Nguyen Thierry
J. J. Brown

Work Performed Under Contract No.: DE-FG22-94PC94224

For
U.S. Department of Energy
Office of Fossil Energy
Federal Energy Technology Center
P.O. Box 880
Morgantown, West Virginia 26507-0880

By
Department of Materials Science & Engineering
Virginia Polytechnic Institute and State University
Blacksburg, Virginia 24061

Disclaimer

This report was prepared as an account of work sponsored by an agency of the United States Government. Neither the United States Government nor any agency thereof, nor any of their employees, makes any warranty, express or implied, or assumes any legal liability or responsibility for the accuracy, completeness, or usefulness of any information, apparatus, product, or process disclosed, or represents that its use would not infringe privately owned rights. Reference herein to any specific commercial product, process, or service by trade name, trademark, manufacturer, or otherwise does not necessarily constitute or imply its endorsement, recommendation, or favoring by the United States Government or any agency thereof. The views and opinions of authors expressed herein do not necessarily state or reflect those of the United States Government or any agency thereof.

HIGH TEMPERATURE ALKALI CORROSION OF DENSE Si_3N_4 COATED WITH CMZP AND Mg-DOPED Al_2TiO_5 IN COAL GAS

Report # 14
for the period
November 1, 1997 -March 1, 1998

Prepared by

Nguyen Thierry and J. J. Brown

Department of Materials Science and Engineering
Virginia Polytechnic Institute and State University
Blacksburg, Virginia 24061

Prepared for

Grant # DE-FG22-94PC94224 -14

Department of Energy
Pittsburgh Energy Technology Center
P.O. Box 10940
Pittsburgh, Pennsylvania 15236

March 1, 1998

U.S. DOE Patent Clearance is not required prior to
the publication of this document.

Over the past twenty years silicon based ceramics have generated considerable enthusiasm in the scientific community. Of particular interest is Si_3N_4, one of the leading candidates of this family, for very demanding structural applications. Its properties are well known and include a high strength to weight ratio, a high chemical resistance, and excellent high temperature properties. However, it was reported in previous papers that the performances of Si_3N_4 were dramatically affected by hot alkali molten salts. In order to alleviate this phenomenon, it was suggested that certain oxide ceramics, which exhibit better resistance to the alkali corrosion, could be applied as protective coatings. Using the sol-gel process and dip coating technique, CMZP and Mg-doped Al_2TiO_5 thin films were deposited on Si_3N_4 substrates and exposure to a sodium containing atmosphere was carried out. During this reporting period, the emphasis was placed on investigating the microstrutural changes of coated and uncoated samples as well as on assessing their alkali corrosion resistance.

EXPERIMENTAL PROCEDURE

Commercially available hot pressed Si_3N_4 with Al_2O_3 and Y_2O_3 sintering additives was used in this study. Corrosion tests, strength degradation, aging tests, and weight loss measurements were performed on modulus of rupture (MOR) bars. Prior to the corrosion test each specimen was heated to 200°C and dipped in a $NaNO_3$ saturated aqueous solution. The amount of salt adhering to the surface was calculated to be 3-4 mg/cm^2. The effect of the alkali corrosion on the mechanical properties of as received and coated Si_3N_4 specimens was examined by 4 point bending using an ATS model 1120 universal testing machine. Five coupons with dimensions 3 x 4 x 50 mm and representing each coating were first exposed to an atmosphere containing a constant 8 vol.% $NaNO_3$ at 1000°C for 96 h. A scheme of the apparatus used for the alkali corrosion experiment is given in Figure 1. Then the room temperature 4 point flexural strength tests were performed at a crosshead of 0.5 mm/min with inner and outer spans of 20 and 40 mm, respectively.

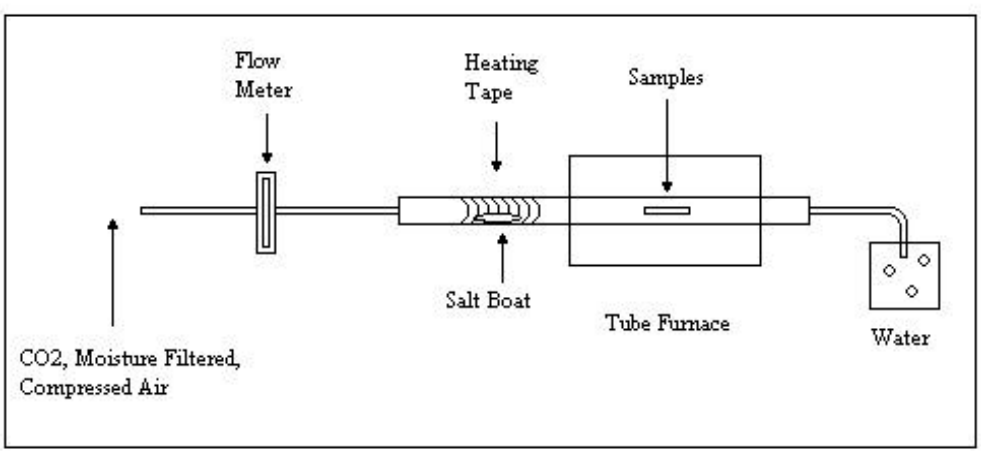

Figure 1 : Schematic of the apparatus devised by G. R. Pickrell for the corrosion test.

To investigate the strength degradation as a function of time, a 1000°C and 360-hour corrosion experiment was conducted. The samples were placed in a furnace where the alkali vapor concentration was calculated to be 4-5 vol%. A scheme of the furnace is given in Figure 2.

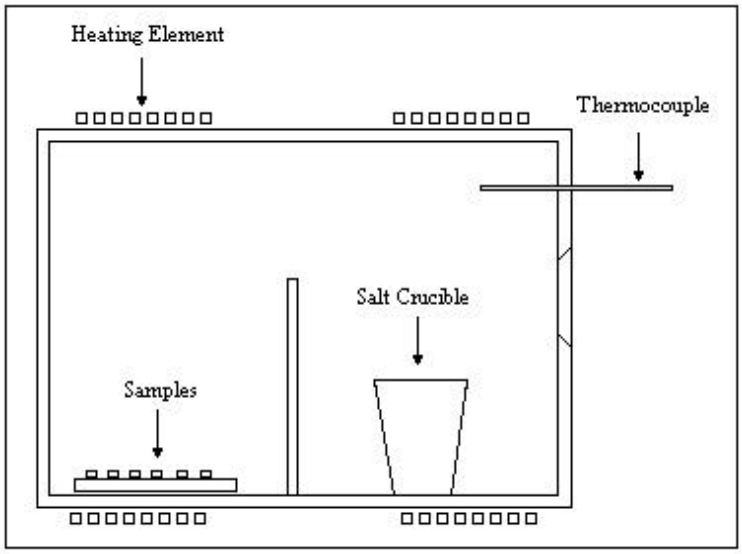

Figure 2 : Schematic of the apparatus used for the aging test.

Every 72 hours three MOR bars with dimension 3 x 4 x 25 mm were cooled down to ambient temperature and their flexural strength was measured by 3 point bending. The bend test had an outer span of 20 mm, an inner span of 10 mm, and a loading rate of 0.2 mm/min. To study the weight loss after corrosion, the specimens were first washed in distilled water at 100°C to remove water soluble phases such as residual salts and sodium silicates, and then etched in 10% HF to remove the corrosion product layer prior to weighing[1].

RESULT AND DISCUSSION

Coatings

The microstructures of Si_3N_4 as received and Si_3N_4 coated with CMZP and Mg-doped Al_2TiO_5 are depicted in Figure 3. Homogeneous and crack free thin film were obtained with the sol-gel process and dip coating technique. CMZP coating features an uneven surface composed of 1-3 μm spheroid grains while Mg-doped Al_2TiO_5 coating formed an aluminum titanium yttrium silicate glassy phase with needle-like particles of yttrium dissilicate at the surface. These needle-like particles have also been observed by other investigators and are the result of the oxidation of yttria, which diffuses from the grain boundary to the surface. The driving force for the diffusion is the necessity to equilibrate the chemical composition of the glassy phase formed[2].

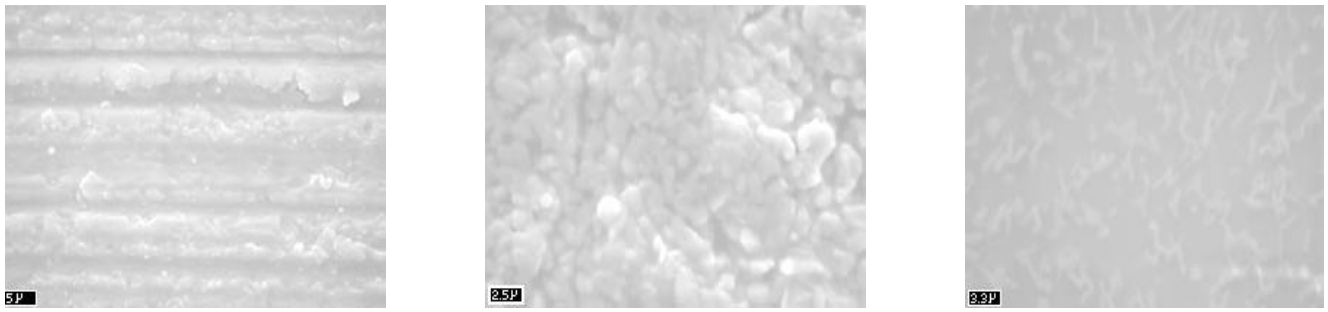

(a) (b) (c)

Figure 3 : SEM surface micrograph of a) Si_3N_4 as received, b) Si_3N_4 coated with CMZP, c) Si_3N_4 coated with Mg-doped Al_2TiO_5.

Cross sections and corresponding elemental mappings of each coated specimen are shown in Figures 4, 5, and 6, respectively. For the as received specimen, EDX mappings indicate the formation of a 1 μm thick silica layer. This silica layer is, however, not pure since Al and Y elements were also detected near the surface. D. S. Fox and N. S. Jacobson have suggested that in the presence of additives, the silica layer acted as a sink for impurities leading to the formation of a glass phase with higher oxygen permeability.[3] The CMZP coating was also observed to be around 1 μm thick. The possibility of a substantial reaction between CMZP, SiO_2, Al_2O_3, and Y_2O_3 is not excluded since Si, Al, and Y elements were also detected at the surface. This would account for the fact that CMZP peaks have never been clearly yielded by XRD. Besides, Ca and Mg were detected in the bulk of the ceramic, suggesting a diffusional process most likely along the grain boundary. For Mg-doped Al_2TiO_5 coating, x-ray maps support the hypothesis of an aluminum titanium yttrium silicate phase. The thickness of the glassy phase was found to range from 2 to 3 μm. As noticed with CMZP, inward diffusion of Mg and Ti along the grain boundary also took place.

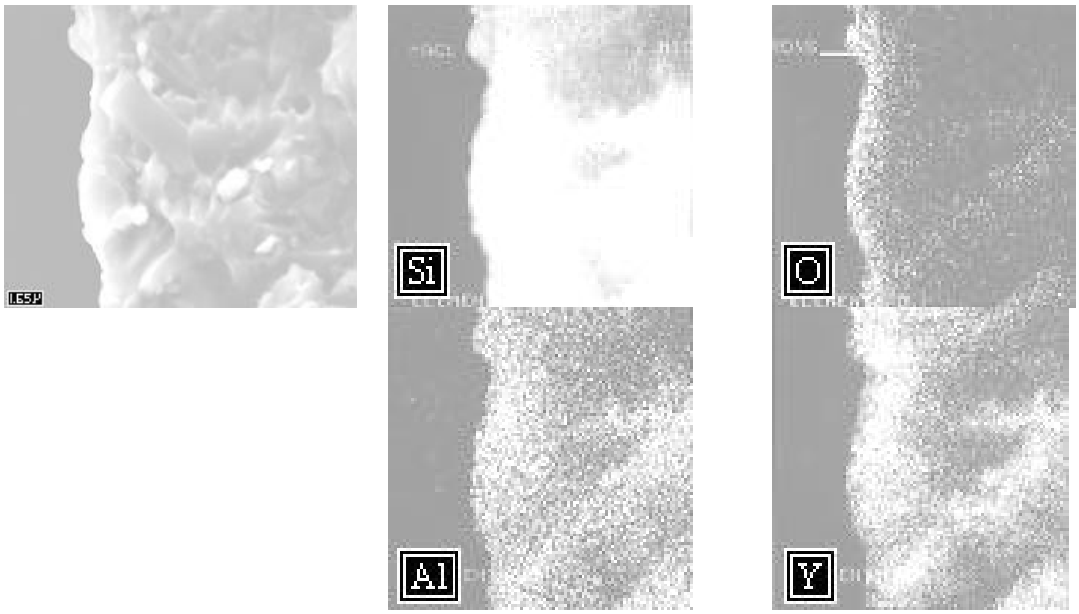

Figure 4 : SEM photomicrograph of a fractured surface for as received Si_3N_4 and corresponding elemental mappings.

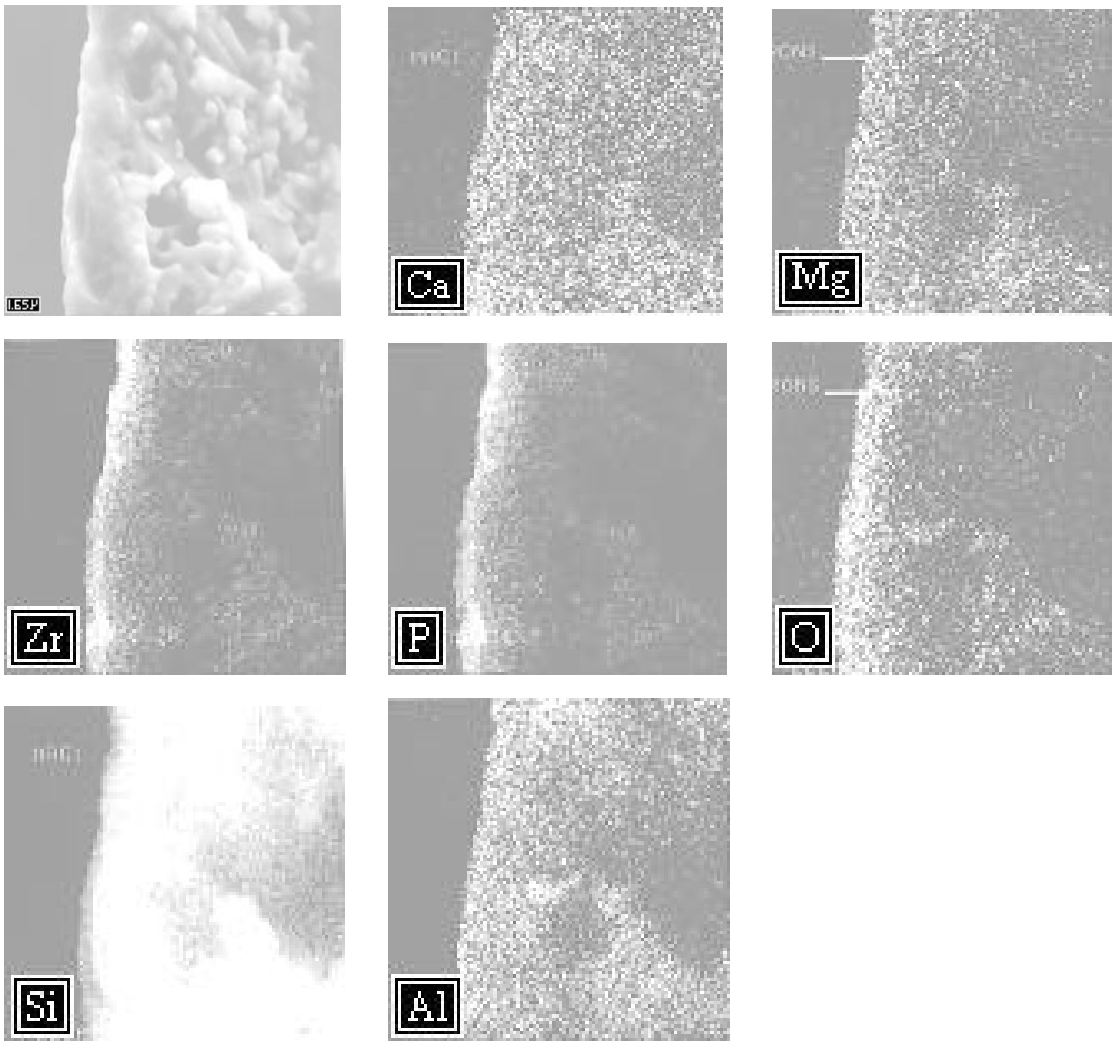

Figure 5 : SEM photomicrograph of a fractured surface for Si_3N_4 coated with CMZP and corresponding elemental mappings.

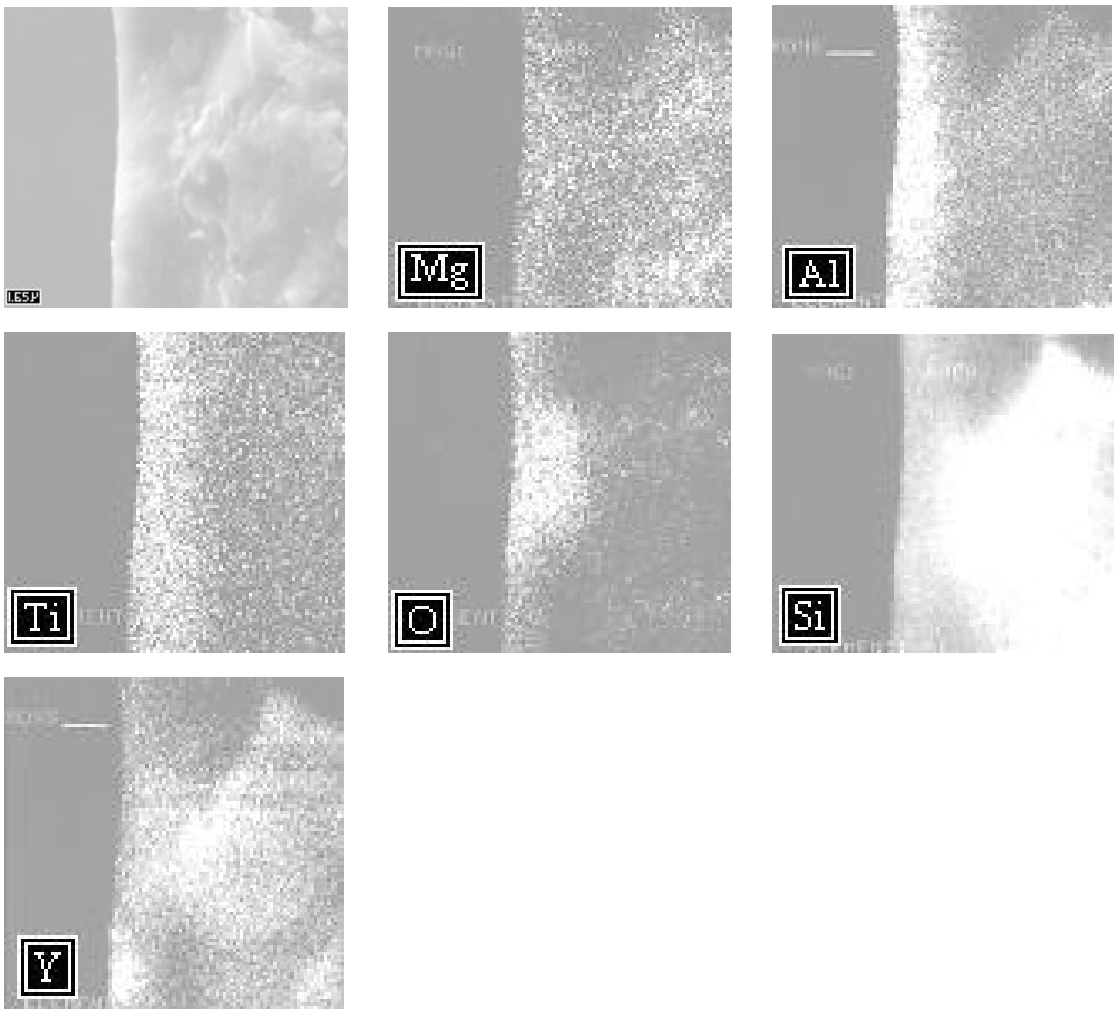

Figure 6 : SEM photomicrograph of a fractured surface for $_3N_4$ coated with Mg-doped Al_2TiO_5 and corresponding elemental mappings.

Effect of the Corrosion Reaction on the Microstructure

At this point in time, it is well known to researchers that Si_3N_4 ceramics are unstable in oxygen and that they rely on a thin film of SiO_2 for oxidation protection. Unfortunately, it was discovered that the cristobalite protective layer underwent fast dissolution when subjected to high temperature alkali containing atmospheres, exposing Si_3N_4 to severe attack. The corrosion mechanism in the presence of sodium compounds has been widely studied[4,5] and consists of a series of step reactions involving first the dissolution of the solid silica film to form a liquid, non-protective sodium silicate layer as shown in reaction (1). Then the reaction proceeds by oxidation of the Si_3N_4 ceramic through inward diffusion of oxygen and outward diffusion of N_2 gas product according to reaction (2). The silica layer formed after oxidation dissolves readily in contact with the sodium silicate phase as can be seen from reaction (3) and from that point the corrosion reaction goes on with the repetition of steps (2) and (3).

$$Na_2O + x\ SiO_2 \Leftrightarrow Na_2O.x\ SiO_2 \qquad (1)$$

$$Si_3N_4 + 3O_2 \Leftrightarrow 3\ SiO_2 + 2\ N_2 \qquad (2)$$

$$SiO_2 + Na_2O.x\ SiO_2 \Leftrightarrow Na_2O.(x+1)\ SiO_2 \qquad (3)$$

To alleviate or minimize the corrosion reaction, it is believed that the refractoriness of the sodium silicate layer should be increased. This can be achieved by introducing other compounds in the reaction layer via the application of a coating prior to corrosion. After the alkali corrosion, two different morphologies were evidenced depending upon the testing procedure. Indeed, for specimens tested with the apparatus devised by G. Pickrell (see Figure 1), a rough corroded surface without a distinct glassy phase was observed. It has been analyzed in the previous report and will not be further discussed here. In contrast, MOR bars tested with the apparatus shown in Figure 2 witnessed the presence of a thick glassy corrosion phase, which suggests the formation of a liquid at the oxidation temperature. The morphologies of the corroded samples examined by SEM were similar for coated and uncoated Si_3N_4. The glassy phase is depicted in Figure 7. The release of gases is clearly evidenced by the presence of holes at the surface. These holes are produced by the evolution of N_2 gas escaping through the corrosion layer as bubbles. These bubbles are 1-20μm in diameter and are observed for all samples.

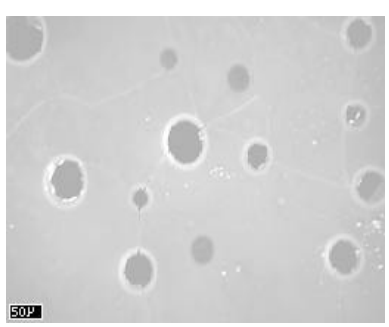

Figure 7 : Morphology of the glassy corrosion product common to coated and uncoated specimens.

For Si_3N_4 as received specimens, the associated x-ray maps yielded an even distribution of Si, O, Al, and Na, (see Figure 8) indicating the formation of a sodium aluminum silicate phase containing a relatively small quantity of Y. For CMZP coating, the corrosion scale was formed of a sodium silicate phase with great amount of Al, Zr and P. Ca, Mg, and Y were also incorporated in the film but to a lesser extent as indicated in Figure 9. For Mg-doped Al_2TiO_5 coating, it was determined from Si, O, Al and Na maps that the corrosion layer consisted primarily of a sodium aluminum silicate phase with a small quantity of Mg, Ti, and Y as depicted in Figure 10. These observations proved that the incorporation of particular compounds in the corrosion scale was successfully attained via the application of sol-gel thin films.

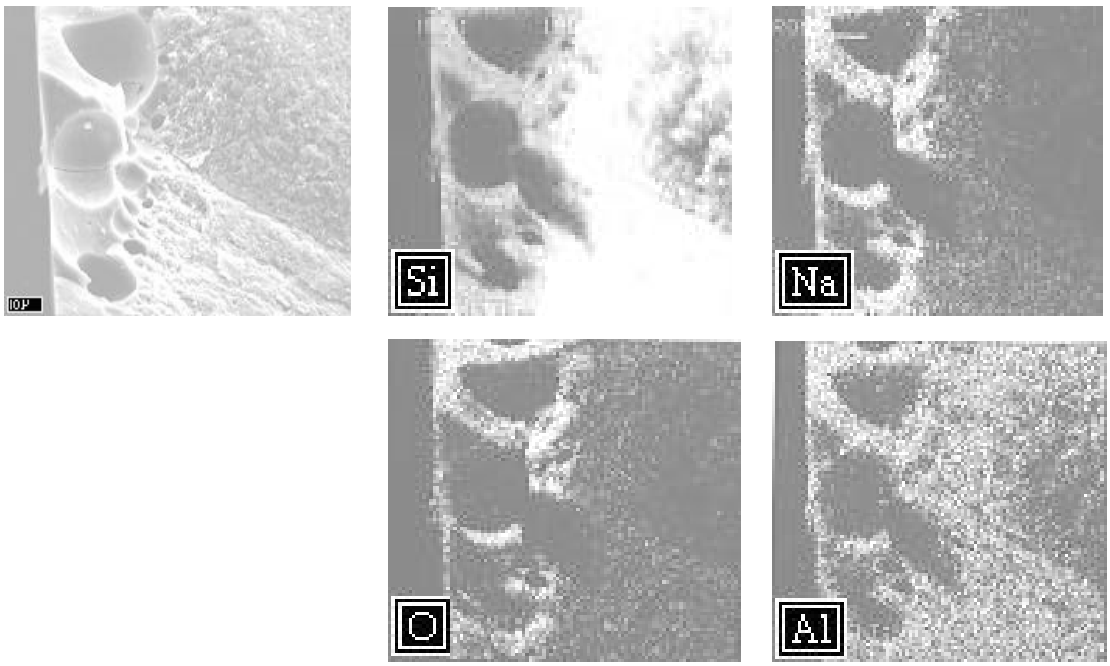

Figure 8 : Fractography and corresponding EDX mappings of as received Si_3N_4 after 216 hour corrosion at 1000°C.

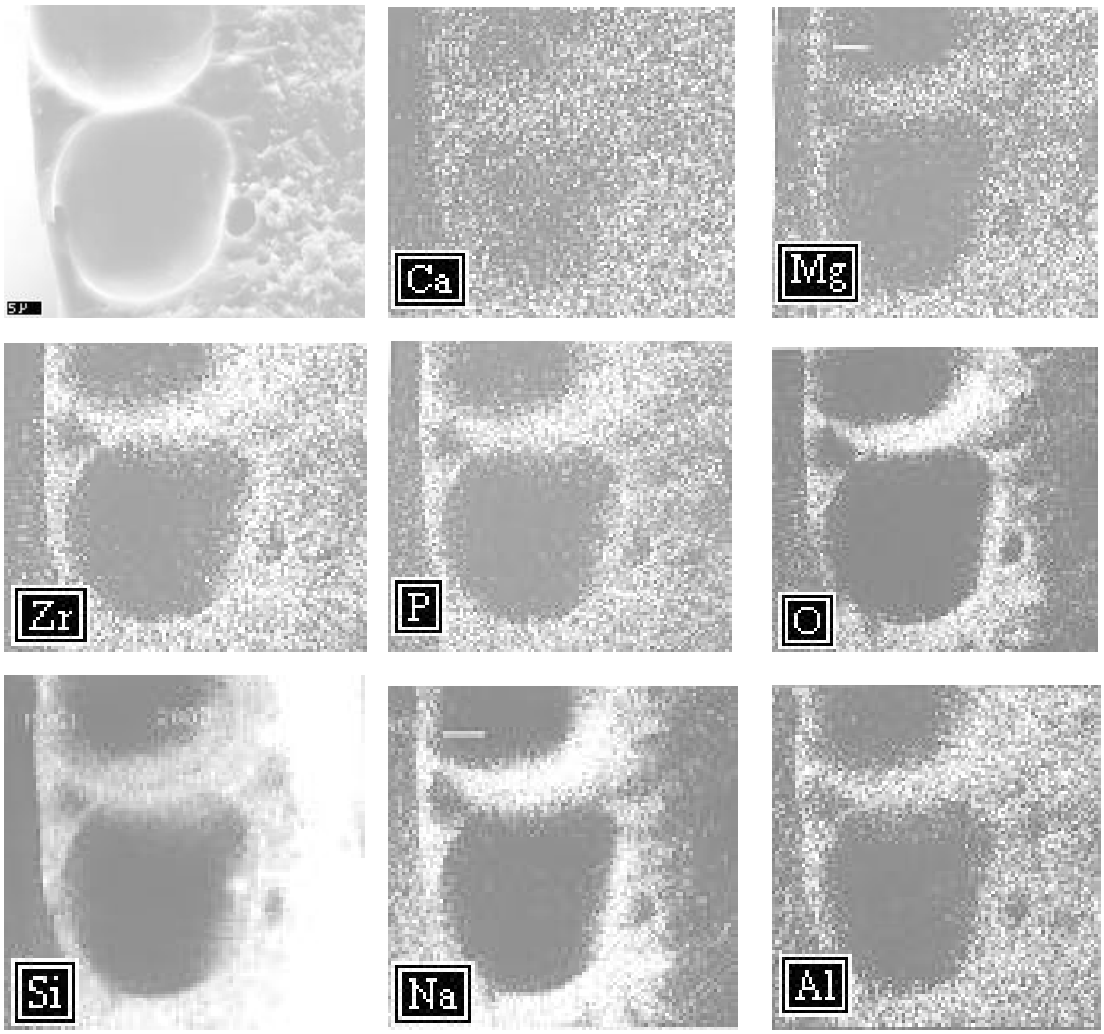

Figure 9 : Fractography and corresponding EDX mappings Si_3N_4 coated with CMZP after 216 hour corrosion at 1000°C.

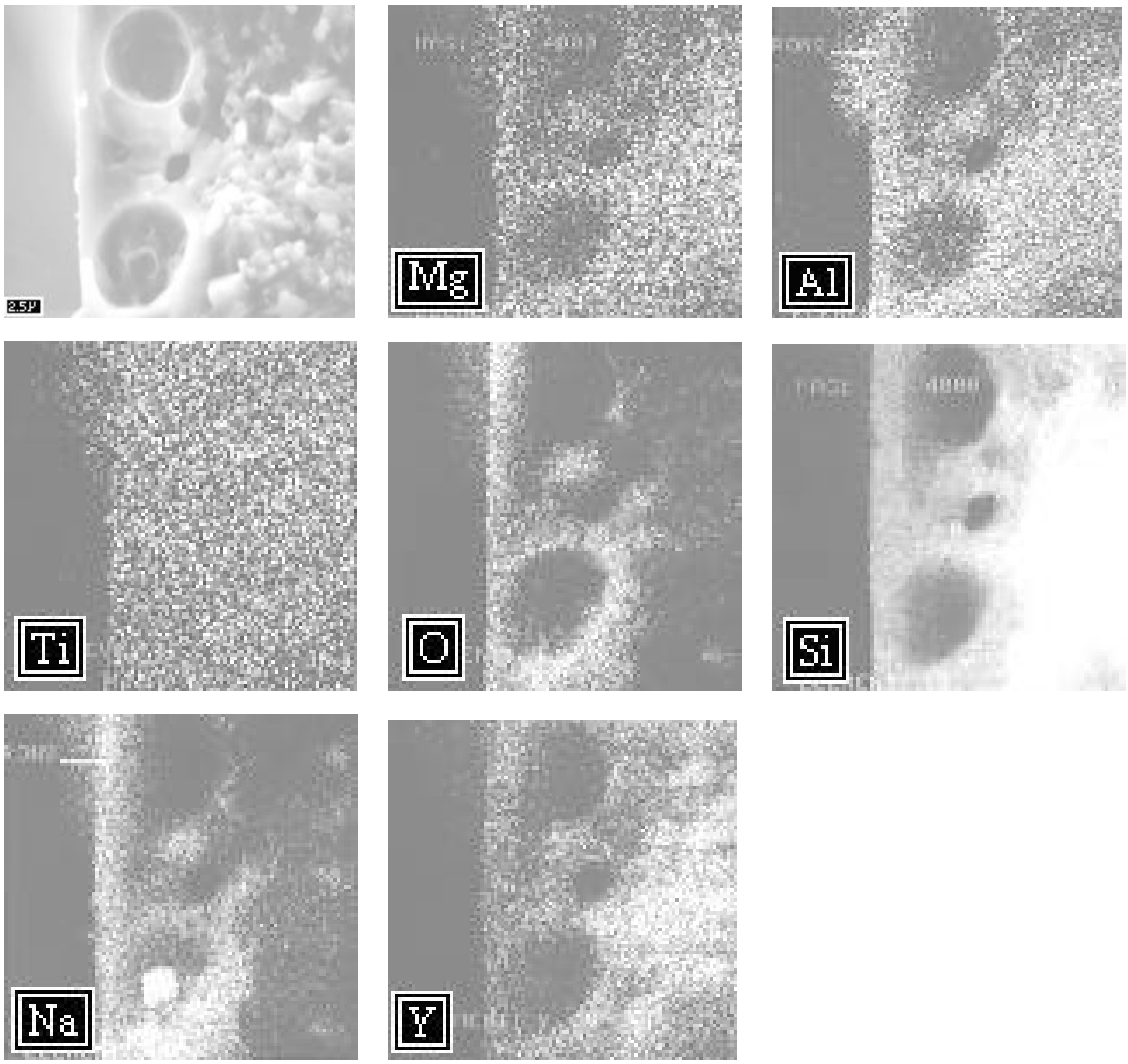

Figure 10 : Fractography and corresponding EDX mappings of $_3N_4$ coated with Mg-doped Al_2TiO_5 after 216 hour corrosion at 1000°C.

In the next step the mode of attack of Si_3N_4 ceramics was investigated. In order to assess whether the corrosion proceeds via uniform surface recession or via enhanced attack in localized regions, the microstructure of the ceramics was examined after removal of the corrosion product by a dilute HF treatment. SEM inspection indicated that only a few bubbles were correlated with some pits as shown in Figure 11. It was observed that the pitting phenomena was of relatively limited importance compared to the uniform surface recession mechanism. This mode of attack reported by other researchers for Si_3N_4 results in the consumption of the ceramic at the grain boundary phase.[6] It is proposed that accelerated chemical reactions are favored by the aggregation of Al_2O_3 and Y_2O_3 which act as softening agents by lowering the solidus temperature of the grain boundary phase[7].

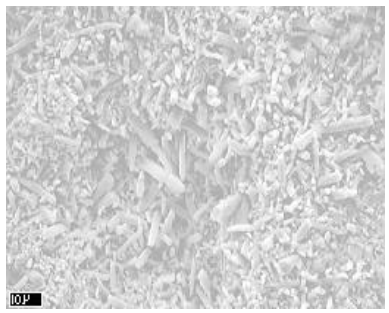

Figure 11 : Typical microstructure of corroded Si_3N_4 after HF treatment.

Alkali Corrosion Resistance

The influence of the alkali corrosion on the fracture strengths of silicon-based ceramics is assessed in this section. Strength degradation of Si_3N_4 in harsh environments is of prime concern because it can set serious limitations on their use in structural applications. The 4 point bend fracture strengths of coated and uncoated specimens before and after 96 hour exposure to sodium vapors are presented in Figure 12 and Table I. As can be seen, the application of the coatings did not significantly affect the strength of Si_3N_4. However, after the corrosion test the strength of all the samples was found to decrease below their initial values. The standard deviation error presented in Table I and calculated with the student's t test, for a level of confidence of 95%, indicates that the strength reductions observed are significant. A comparison of the three sets of specimens with uncoated Si_3N_4 taken as reference show the least strength degradation for CMZP. On the other hand, the formation of an aluminum titanium yttrium silicate glassy phase has, to a large extent, affected the mechanical properties of Si_3N_4.

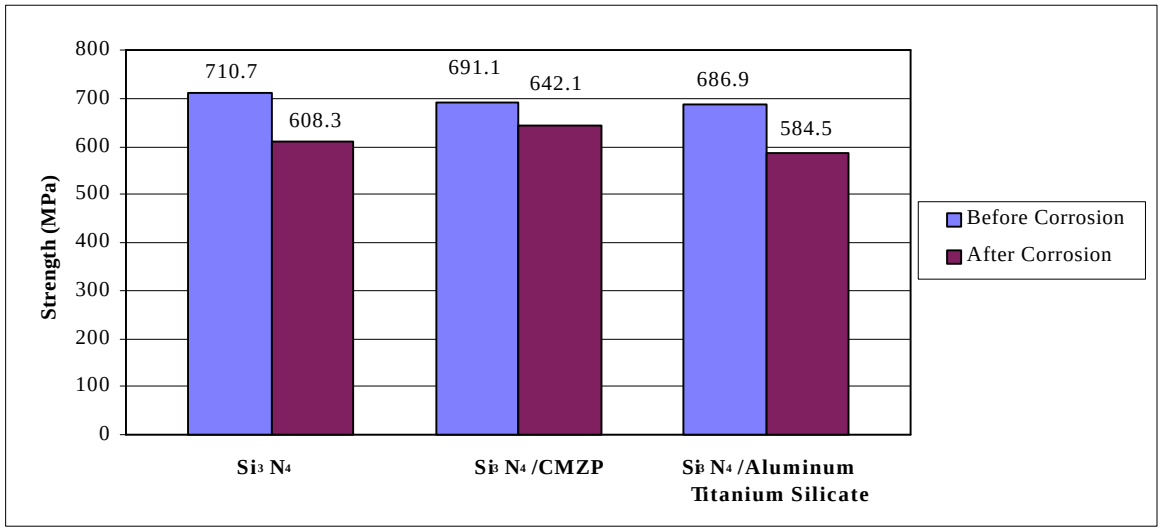

Figure 12 : Strength of coated and uncoated Si_3N_4 before and after 96 hour corrosion at 1000°C.

	Strength (MPa)		
	Si_3N_4	**CMZP**	**Mg-doped Al_2TiO_5**
Before Corrosion	710.7 ± 15.6	691.1 ± 12.7	686.9 ± 15.1
After Corrosion	608.3 ± 13.2	642.1 ± 13.8	584.5 ± 18.8

Table I : Alkali corrosion resistance of coatings.

The 3 point bend flexural strength and weight loss measurements as a function of time were also investigated and are shown in Figures 13 and 14, respectively. The same trend as with the 4 point bending test was observed. With regard to both strength degradation and weight loss, CMZP exhibited the best behavior after aging, followed by Si_3N_4 as received and Si_3N_4 coated with Mg-doped Al_2TiO_5. These results tend to indicate that the incorporation of Ca, Mg, Zr, and P in the corrosion scale resulted in a more refractive layer, which could impede the corrosion process. Conversely, the addition of Al, Mg, and Ti in the corrosion products seems to have the opposite effect, indicating the promotion of the oxygen diffusivity throughout the reaction scale. To further understand the strength degradation from a mechanical standpoint, the fracture surface of broken specimens was examined. In all cases it appeared that the source of failure originated from the lenticular occlusions created by trapped bubbles. It was observed that the brittle failure occurred upon extension of these bubbles, which acted like large pores.

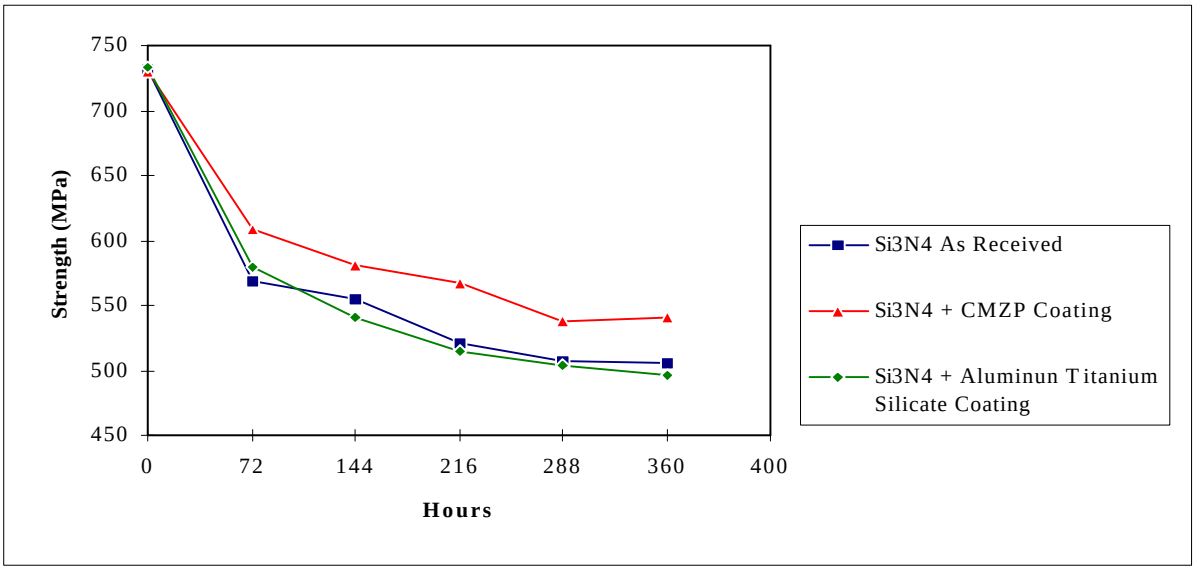

Figure 13 : 3 point bend flexural strength as a function of time after sodium vapor corrosion at 1000°C.

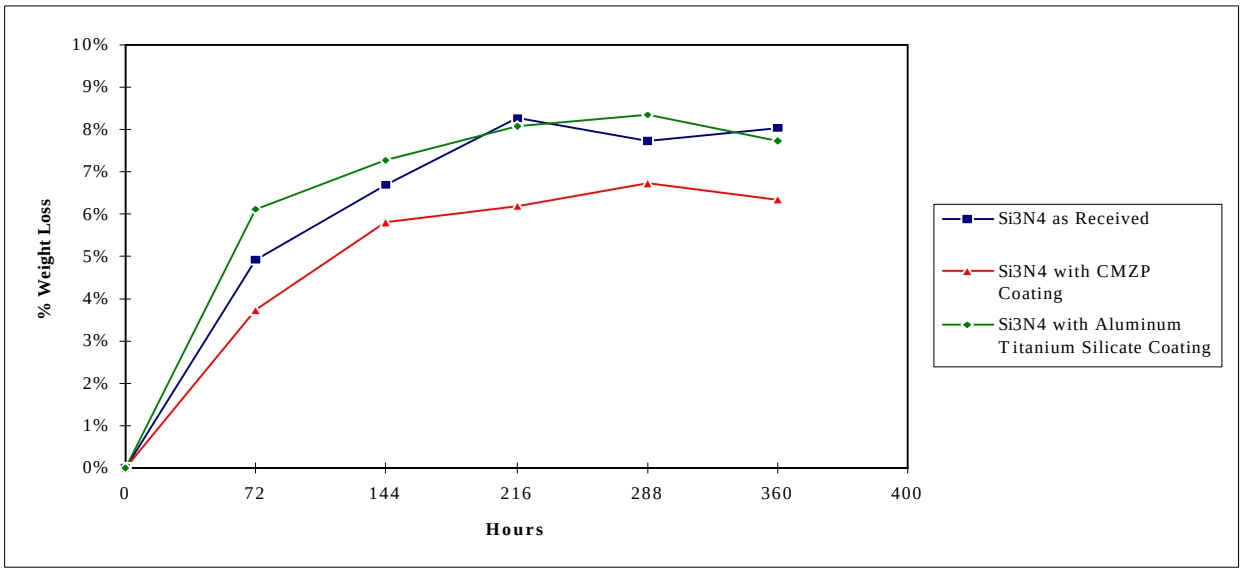

Figure 14 : Weight loss measurements as a function after sodium vapor corrosion at 1000°C.

BIBLIOGRAPHY

[1] : T.K. Li et al., "Thin Film Coatings of $(Ca_{0.6},Mg_{0.4})Zr_4(PO_4)_6$ (CMZP) on Si_3N_4 and SiC," *J. Mat. Res.*, **8**, [11] (1993).

[2] : G. N. Babini et al, "Factors Influencing Structural Evolution in the Oxide of Hot-Pressed Si_3N_4-Y_2O_3-SiO_2 Materials,"*J. of Mat. Sc.*, **19**, 3487-3497 (1984).

[3] : D. S. Fox et al, "Molten Salt Corrosion of Silicon Nitride: I, Sodium Carbonate," *J. Am. Ceram. Soc.*, **71** [2] 128-38 (1988).

[4] : T. Sato et al. "Corrosion of Si_3N_4 in Molten Alkali Sulfate and Carbonate," *Advan. Cera. Mat.* **2**, [3A] 228-31 (1987).

[5] : Shaokai Y., "Corrosion Resistant CMZP and Mg-Doped Al_2TiO_5 Coatings for SiC Ceramics," Master's Thesis, Dept. Materials Science and Engineering, Virginia Tech (1996).

[6] : N. S. Jacobson, J. L. Smialek et al, "Molten Salt Corrosion of SiC and Si_3N_4," *Handbook of Ceramics and Composites*, **1**, (1990).

[7] : G. R. Pickrell, T. Sun et al, "High Temperature Alkali Corrosion of SiC and Si_3N_4," *Fuel Processing Technology*, **44**, 213-236 (1995).